International Journal of Mechanical and Materials Engineering (IJMME), Vol. 7 (2012), No. 3, 186-191.

AN EXPERIMENTAL INVESTIGATION OF THE EFFECT OF THE MULTI VORTEX GENERATOR FOR DRAG REDUCTION IN A UTILITY VEHICLE

P. Gopal and T. Senthilkumar*
Department of Automobile Engineering, University College of Engineering, BIT Campus, Tiruchirappalli, India.
*Corresponding author's E-mail: gopal_pp@rediffmail.com

Received 25 January 2012, Accepted 18 December 2012

ABSTRACT
An experimental investigation was done in a subsonic wind tunnel to study the variation of drag and lift with and without multi vortex generators (MVG) on the roof of a utility vehicle at varying length to height ratio of MVG. The length to height (L/H) ratio used are 1.5, 2 and 2.5.To measure the effect of altering the vehicle body, wind tunnel tests have been performed with 1:15 scaled model of the utility vehicle with velocities of 2.42, 3.7, 5.42 and 7.14 m/s. The experiments showed that a great improvement of the aerodynamic drag force reduction can be achieved with multi vortex generator.

Keywords: Aerodynamics, Multi vortex generator, Drag, Lift, Wind tunnel.

NOMENCLATURE

Re	Reynolds Number (Dimensionless)
$U\infty$	Free Stream Velocity of Air (m/s)
ρ	Density of Air (kg/m^3)
A	Projected Area (m^2)
S	Distance Travelled by vehicle (m)
Cp	Pressure Coefficient (Dimensionless)
u	Local velocity of air (m/s)
P	Static pressure (N/m^2)
$P\infty$	Total Pressure (N/m^2)
P_d	Dynamic Pressure (N/m^2)
C_D	Coefficient of drag (Dimensionless)
C_L	Coefficient of lift (Dimensionless)

1. INTRODUCTION

A multi vortex generator is an aerodynamic surface which is basically a small vane that creates a vortex. They can be found in many systems like aircraft, ships, turbines, ground vehicles etc. Multi vortex generators are added to maintain steady airflow over the control surfaces at the rear of the airplane wing. They are typically rectangular or triangular in shape and about 1 or 2 cm in size (Williamson, 1996). There have been recent developments in using multi vortex generators for passive control of shock/boundary-layer interactions, involving both experiment and computation. The precise mechanism of how they function at high speeds remains the subject of debate (Alam and Watkins, 2004; Hucho, 1998; Cooper, 2006; Barlow et al., 1999; RAS, 1981; Stephens, 1957; Kuethe, 1970; Wheeler, 1991). Many different stepped cavitators moving with high speed in the water to find those with lower drag force were also numerically investigated by Mobini (2012). Similarly a numerical study of vortex generators in a low speed flow has been done by Ahmad (2011).

Studies indicate that multi vortex generators modify the inner structure of the boundary layer to make the layer more resistant to separation. Some investigators suggest that the trailing vortices provide the mixing with the free stream to energize the boundary layer. However, apparently no experimental or computational results have been obtained to support this suggestion. A practical advantage of multi vortex generators is their small size which results in less drag than their conventional counterparts (Landman et al., 2009; Schoon, 2007; Watkins et al., 1987; Snyder, 1977).

The primary objective of this study is to investigate the aerodynamic effects of adding multi vortex generator (MVG) and their impact on fuel consumption. For a motor vehicle travelling at a constant velocity on a level road, the power required to overcome the aerodynamic drag is approximately 80%) and that for the tyre rolling resistance is around 20%. However, with an increase of speed, the required power increases significantly to overcome aerodynamic resistance (drag) while the power required for rolling resistance remains almost constant (Clark and Dodge, 1979).

$$\text{Power}_{(\text{Required})} = C_D \tfrac{1}{2} \rho A V^3 \quad (1)$$

Although the primary focus of vehicle manufacturers and researchers have been concentrated on fuel saving devices of the commercial vehicles till to date, it has also become important to study the aerodynamic effects on fuel consumption of utility vehicle (Zulfaa and Antonio, 2010). Hence**,** in this work, the variations of pressure coefficient and dynamic pressure on the roof of a utility vehicle with and without multi vortex generators (MVG) have been investigated. The effect of various L/H ratios (length to height ratio) of MVG on pressure coefficient and dynamic pressure is also presented.

2. EXPERIMENTAL DETAILS

2.1 Design of MVG

Delta shaped MVG's were most commonly used on aircraft wings because of their simplicity in design, ease of mounting and lower drag (Masar et al., 2004). Hence, in this work, a single vane delta (triangular) shaped VG is chosen. In order to find a viable configuration, one

must first identify the important variables for MVG design. In order to reduce the degrees of freedom, most of the variables were fixed based on either analysis or recommendations of previous researchers (Volkswagen, 2009). In connection with the height, the thickness of the boundary layer is measured based on the assumption that the optimum height of the MVG would be nearly equal to the boundary layer thickness. Figure 1 shows the velocity profile on the vehicle's roof. From Figure 1, the boundary layer thickness at the roof end immediately in front of the separation point is found to be about 2 mm. This reveals that the optimum height of the MVG must not be less than 2 mm. Consequently, the optimum height for the MVG is fixed at 2 mm. The thickness of MVG was fixed at 0.5 mm uniform throughout so as to make a stiffened structure.

Length was taken in proportion of the height of the MVG. In this experimental work, three values of L/H ratio was taken as 1.5, 2 and 2.5. The parameter "interval" describes the spacing between MVG in a row. The ratio of interval length of VGs to height (I/H ratio) is taken as 6. Based on this I/H ratio, a single row of MVG was positioned on the roof with 8 numbers of MVG. Based on the boundary layer measurements and separation point of the stream line on the roof, one row of MVG was mounted at a distance of 5 mm from the roof end.

The number of row was limited to one in order to minimize weight and potential manufacturing cost. The delta shaped MVGs are installed at a yaw angle of 15° to the airflow direction. But the airflow direction was found to be different between sideways positions on the roof.

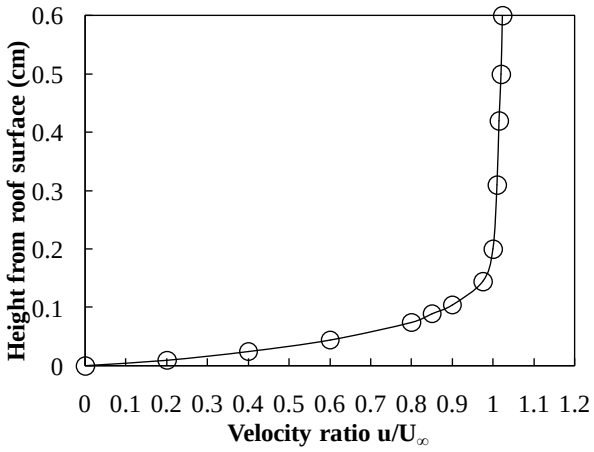

Figure 1 Velocity profile on roof.

The airflow is aligned directly with the backward direction at center of a vehicle, but it increasingly deviates toward the center as the measurement point shifts away from the central position. For this reason, the delta-wing-shaped MVGs must be installed at an angle of 15° against the vehicle centerline for the central position, whereas they must be installed at an angle near 0° for outermost positions. The arrangement of MVG is shown in Figures 2(a) and (b).

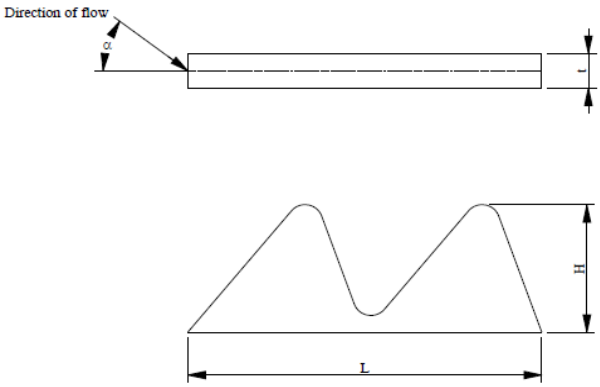

Figure 2(a) Dimensions of MVG.

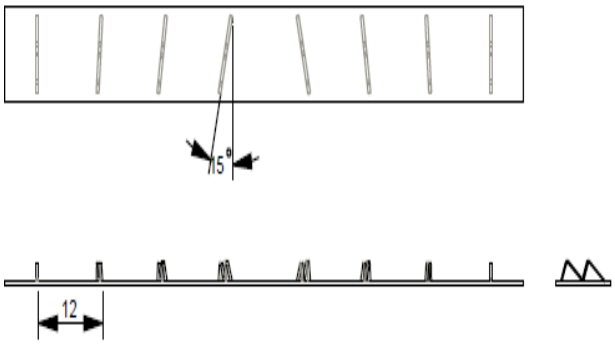

Figure 2 (b) Arrangement of MVG in a row.

2.2 Scale model and wind tunnel test facility

The test model used was Tata Sumo Grande with a scale ratio of 1:15. The scale model of the vehicle is shown in Figure 3.

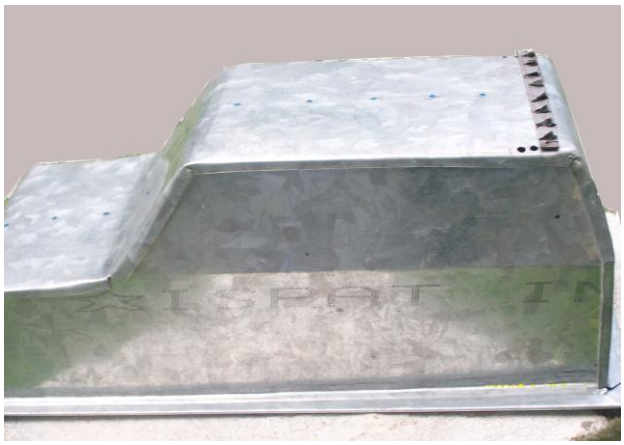

Figure 3 Scale Model.

The length, breadth and height of the scaled model are 0.295 m, 0.108m and 0.1m respectively. Thickness of the sheet metal used was 0.5mm.The Multi Vortex generators were cut into pieces from the sheet metal and they were fixed on to a base plate by gas welding process. The base plate with MVG was fastened to the roof of scaled model by means of bolt and nut as shown in Figure 3.

To measure the static pressure on the body, 0.2 mm diameter holes were drilled on the centre line of the vehicle body starting from the front end along the roof to the rear end of the vehicle. 15 pressure tappings are used. Out of which five of them are on the roof, three on the rear end and remaining seven are on the front end of the vehicle. Pressure tubes are fixed from inside of the holes. Pressure tappings are connected to micro manometer using pressure tubes. An open circuit wind tunnel (Altech, India) with a test section of 0.09 m^2 was used. The schematic of the wind tunnel is shown in Figure 4.

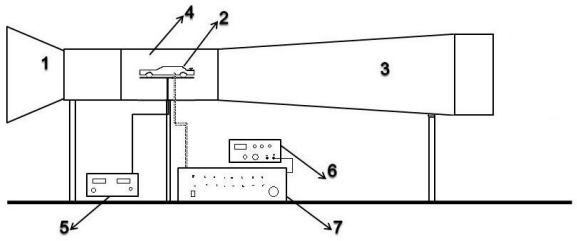

1-Air Filter
2-Car Model
3-Axial Fan Duct
4-Test Section
5-Force Display Unit
6-MicroManometer
7-20 Line Single Way Selection Box

Figure 4 Experimental setup.

The total length of the wind tunnel was 6m and the test section length was 1 m. A 25 HP electric motor was used for suction. The pressure data were not corrected for horizontal buoyancy as the static pressure gradient in the wind tunnel was deemed negligible. The wind tunnel tests were conducted at positive and negative yaw angles between ±15°. The frontal area of the scale model of the vehicle is 0.0108 m^2. The blockage ratio is calculated to be about 9.2%. The relative air speed was measured by using micro manometer (Furnace control ltd, UK) in wind tunnel test section. This relative air speed was measured to calculate the dynamic pressure variations along the centre line of vehicle body. A micro manometer (Honeywell make) has an accuracy of ± 0.5 %. Velocity uniformity is ±0.96% which is less than 1% as given in SAE Wind Tunnel Test procedure (SAE, 1981).

3. DATA REDUCTION

The equations used in the estimations of various non-dimensional terms like pressure coefficient, coefficient of drag, coefficient of lift, static and dynamic pressures can be found in the literature (Hucho, 1998). Uncertainty analysis is carried out using Coleman and Steele (1981) and ANSI/ASME standards (1986) considering the measurement errors whereas the possible errors in the fluid properties are not included. The uncertainty in the measurements of dynamic pressure, pressure coefficient, coefficient of drag and coefficient of lift are calculated using the following equations:

$$\frac{\Delta c_p}{c_p} = \left(\left(\frac{\Delta p_\infty}{p} \right)^2 + \left(\frac{2\Delta u_\infty}{u_\infty} \right)^2 \right)^{0.5} \quad (2)$$

$$\frac{\Delta c_D}{c_D} = \left(\left(\frac{\Delta D}{D} \right)^2 + \left(\frac{2\Delta u_\infty}{u_\infty} \right)^2 + \left(\frac{\Delta A}{A} \right)^2 \right)^{0.5} \quad (3)$$

$$\frac{\Delta c_L}{c_L} = \left(\left(\frac{\Delta L}{L} \right)^2 + \left(\frac{2\Delta u_\infty}{u_\infty} \right)^2 + \left(\frac{\Delta A}{A} \right)^2 \right)^{0.5} \quad (4)$$

The uncertainty is ±1.12% for dynamic pressure and pressure coefficient, ±1.42% C_D and C_L.

4. RESULTS AND DISCUSSIONS

4.1 Pressure coefficient

Figure 5 shows the variation of pressure coefficient along the X coordinates of the scale model at a free stream velocity of 2.42 m/s. From the figure it is observed that the value of pressure coefficient without MVG is minimum at the x coordinate of about 240 mm, whereas its value is maximum with MVG having L/H ratio of 2. This is shown as inset of Figure 5.

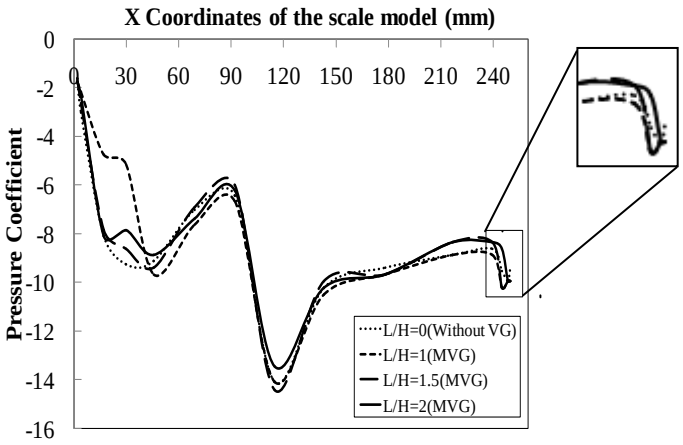

Figure 5 Variation of C_p at U_∞ = 2.42 m/s for different values of L/H ratio.

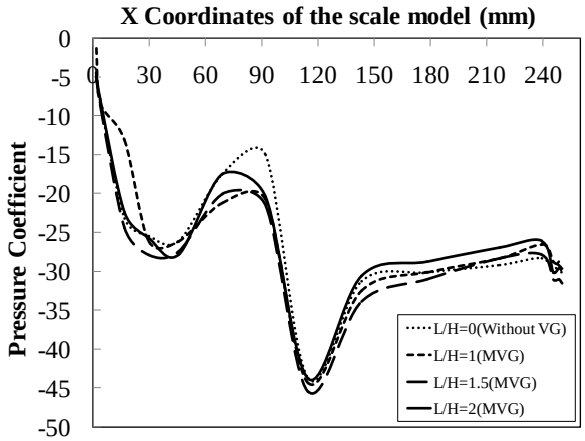

Figure 6 Variation of C_p at U_∞ = 3.7 m/s for different values of L/H ratio.

It is due to the fact that the thickness of the boundary layer is nearly equal to the value of height of MVG at L/H ratio of 2. Figures 6, 7 and 8 show the variation of pressure coefficient along the X coordinates of the scale model at free stream velocities of 3.7, 5.42 and 7.14 m/s respectively. It is evident that the values of pressure coefficient don't change significantly with increase in velocity for various values of L/H ratio. This can be attributed to the fact that the boundary layer thickness is inversely proportional to Reynolds number and hence at higher velocities i.e., at higher Reynolds number the boundary layer thickness becomes too small and hence the effect of L/H ratio of MVG could not be realized. However, it is interesting to observe that the pressure coefficient can be increased with the inclusion of MVG by around 19% at a velocity of 7.14 m/s. Similarly the pressure coefficient can be increased with the inclusion of MVG to a maximum of around 26% and 20 % at a velocity of 5.42 and 3.7 m/s respectively for L/H ratio of 2.

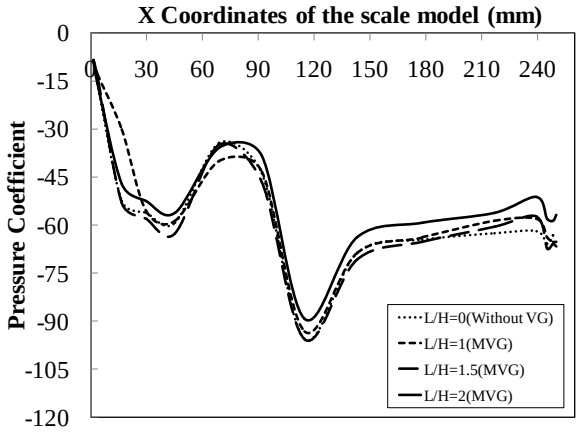

Figure 7 Variation of C_p at U_∞ = 5.42 m/s for different values of L/H ratio.

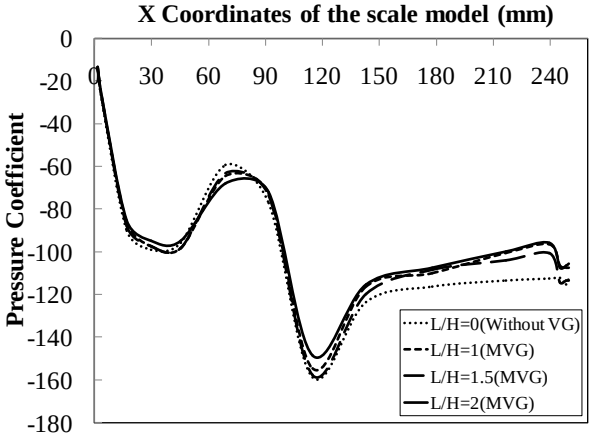

Figure 8 Variation of C_p at U_∞ = 7.14 m/s for different values of L/H ratio.

4.2 Dynamic Pressure

Figure 9 shows the variation of Dynamic pressure along the X coordinates of the scale model at a free stream velocity of 2.42 m/s. From the figure it is observed that the value of dynamic pressure without MVG is maximum at the x coordinate of about 240 mm, whereas its value is minimum with MVG having L/H ratio of 2. The results shows that the dynamic pressure over the surface of the vehicle roof increases with addition of MVG which is favourable for avoiding flow separation and the consequent losses.

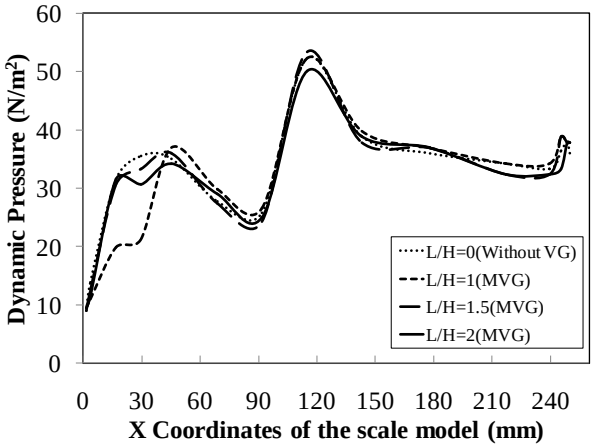

Figure 9 Variation of P_d at U_∞ = 2.42 m/s for different values of L/H ratio.

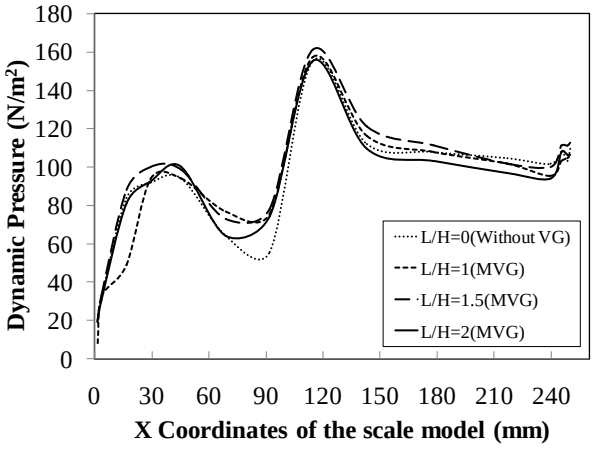

Figure 10 Variation of P_d at U_∞ = 3.7 m/s for different values of L/H ratio.

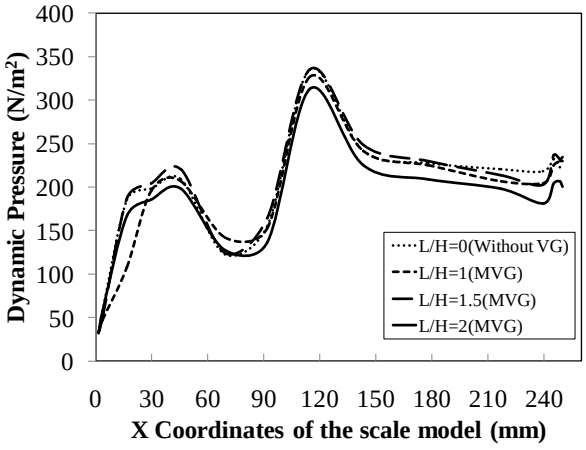

Figure 11 Variation of P_d at U_∞ = 5.42 m/s for different values of L/H ratio.

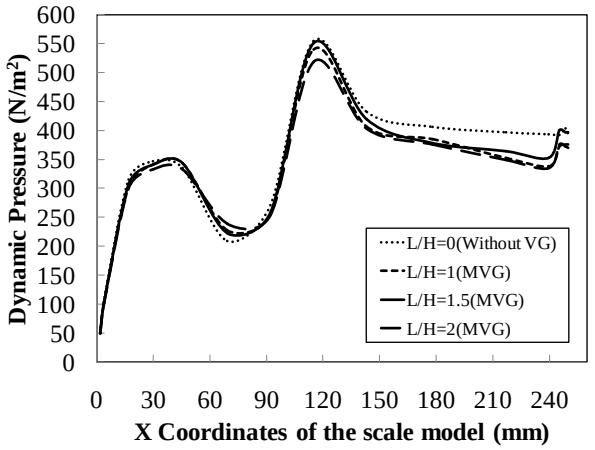

Figure 12 Variation of P_d at U_∞ = 7.14 m/s for different values of L/H ratio.

Figures 10, 11 and 12 shows the variation of dynamic pressure along the X coordinates of the scale model at a free stream velocity of 3.7, 5.42 and 7.14 m/s respectively. It is evident that the values of dynamic pressure don't change significantly with increase in velocity for various values of L/H ratio. However, it is interesting to observe that the dynamic pressure can be increased with the inclusion of MVG by around 19% at a velocity of 7.14 m/s. Similarly the dynamic pressure can be increased with the inclusion of MVG to a maximum of around 24% and 18 % at a velocity of 5.42 and 3.7 m/s respectively for L/H ratio of 2.

4.3 Coefficient of drag

Figure13 shows the variation of C_D values for different values of L/H ratio at varying free stream velocities along the longitudinal centre plane of the scale model.

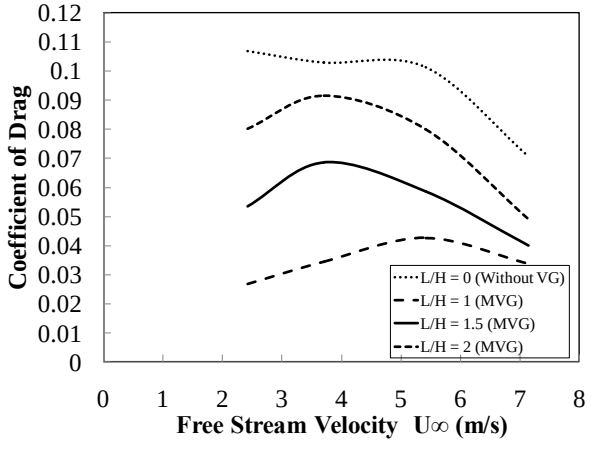

Figure 13 Variation of C_D for different values of L/H ratio.

It is clearly evident from the figure that the value of CD decreases due to the addition of MVG. This can be attributed due to the avoidance of flow separation with the help of MVG. For instance at a velocity of 2.42 m/s the coefficient of drag is reduced by a maximum of 90% when MVG of L/H =2 is used when compared to the values obtained without MVG. Similarly at same velocity a minimum of 18% reduction in drag is obtained for MVG of L/H = 1. For lower L/H ratio, the CD remains constant for increase in velocity. However, when L/H ratio is increased the values of CD varies with increase in velocity. This is due to the reason that with increasing value of velocity, the Reynolds number increases which in turn decreases the boundary layer thickness. Therefore, it is concluded that MVG with higher L/H ratio will be useful at lower velocity.

4.4 Coefficient of lift

Figure14 shows the variation of C_L values for different values of L/H ratio at varying free stream velocities along the longitudinal centre plane of the scale model. It is clearly evident from the figure that the value of C_L decreases due to the addition of MVG. This can be attributed due to the avoidance of flow separation with the help of MVG. For instance at a velocity of 2.42 m/s the coefficient of lift is reduced by a maximum of 89% when MVG of L/H =2 is used when compared to the values obtained without MVG. Similarly at same velocity a minimum of 50% reduction in lift is obtained for MVG of L/H = 1. However the value of C_L decreases with increase in velocity with and without MVG. The results revealed that at higher velocity the value of C_L remains constant for VG of all L/H ratios.

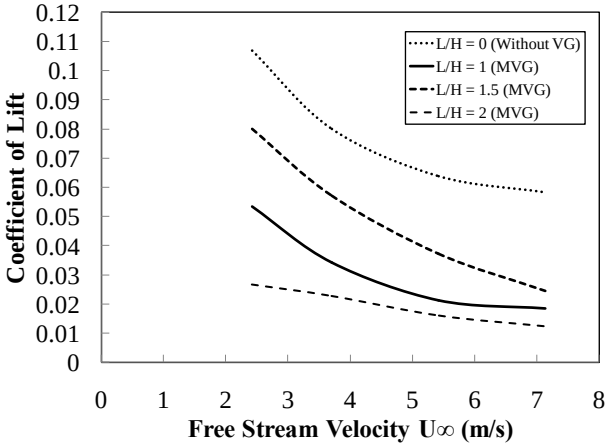

Figure 14 Variation of C_L for different values of L/H ratio.

5. CONCLUSION

From the experimental investigation on the measurement of the variation of pressure coefficient and dynamic pressure on the roof of a utility vehicle with and without multi vortex generators (MVG), the following conclusions were made

(i) The value of pressure coefficient is minimum without MVG whereas its value was observed to be maximum with MVG when the L/H ratio is 2 at which the boundary layer thickness is nearly equal to height of the MVG.

(ii) The pressure coefficient can be increased with the inclusion of MVG by around 19% at a velocity of

7.14 m/s at an x coordinate of 240 mm along the longitudinal plane of the scale model.

(iii) The values of pressure coefficient don't change significantly with increase in velocity for various values of L/H ratio.

(iv) Dynamic pressure over the surface of the vehicle roof increases with addition of MVG which is favourable for avoiding flow separation and the consequent losses.

(v) The value of CD is reduced by 90% with the addition of MVG at a velocity of 2.42 m/s and a minimum of 18% reduction in drag is obtained for MVG of L/H = 1

(vi) It is observed that MVG of higher L/H ratio will be useful at lower velocity

The value of C_L decreases with increase in velocity with and without MVG and the results revealed that at higher velocity the value of C_L remains constant for VG of all L/H ratios.

REFERENCES

Ahmad, K.A. 2011. Numerical Study on Effect of Reduced Frequency on a Vortex Induced by an Oscillating Sub Boundary Layer Vortex Generator, International Journal of Mechanical and Materials Engineering 6 (3): 317-325.

Alam, F. and Watkins, S. 2004. Aerodynamics of Trucks and Drag Reducing Devices, Journal of Mechanical Engineering, International conference on mechanical engineering (ICME09), Khulna University of Engineering and Technology, Khulna, Bangladesh.

ANSI/ASME, 1986. Measurement uncertainty, PTC 19, 1-1985, 1986

Barlow, J.B., Rae, J.W.W. and Pope, A. 1999. Low-Speed Wind Tunnel Testing, Third Edition. John Wiley & Sons, Inc., New York, NY.

Clark, S.K. and Dodge, R.N. 1979. A Hand Book for the rolling resistance of pneumatic tires, Industrial development division, Institute of Science and Technology, The University of Michigan, Ann Arbor.

Coleman, H.W. and W.G. Steele. 1989. Experimental and uncertainty analysis for engineers, Wiley, New York, 1989.

Cooper, K.R. 2006. Full-Scale Wind Tunnel Tests of Production and Prototype, Second-Generation Aerodynamic Drag-Reducing Devices for Tractor-Trailers, SAE Paper No. 2006-01-3456, USA.

Hucho, W.H. 1998. Aerodynamics of Road Vehicles, 4th edition, Society of Automotive Engineers (SAE), Warrendale, USA.

Kuethe, A.M. 1970. Boundary Layer Control of Flow Separation and Heat Exchange, US Patent3,74, 1,285. U.S. Department of Commerce, Washington DC.

Landman, D., Wood, R.M., and Seay, W.S. 2009. Understanding Practical Heavy Truck Drag Reduction Limits, SAE Paper No. 2009-01-2890, USA.

Masar K., Nagayoshi, T. and Hamamoto, N. 2004. Research on aerodynamic drag reduction, Mitsubishi Motors, Technical Review, No.16.

Mobini, K. 2012. Drag Reduction of Submerged Moving Bodies Using Stepped Head Shape, International Journal of Mechanical and Materials Engineering 7 (1): 41–47.

RAS 66029. 1981. Subsonic Performance Data for NACA Type Submerged Air Intakes, Royal Aeronautical Society.

SAE. 1981. Wind Tunnel Test Procedure for Trucks and Buses, Recommended Practice-July 1981- SAE J 1252.

Schoon, R. E. 2007. On-road Evaluation of Devices to Reduce Heavy Truck Aerodynamic Drag, SAE Paper 2007-01-4294, USA.

Stephens, A.V.1957. Solid Boundary Surface for Contact with a Relatively Moving Fluid Medium', U.S.Patent No. 2,800,291. U.S. Department of Commerce, Washington DC.

Snyder, R.H. 1977. Tire Rolling Losses and Fuel Economy, SAE Special Publication, P-74, Detroit, USA.

Volkswagen-New-Polo-Wind-Tunnel-Testing, Image: http://www.carbodydesign.com/archive/ Accessed on: 14/05/2009.

Watkins, S., Saunders, J.W. and Hoffmann, P.H. 1987. Wind Tunnel Modeling of Commercial Vehicle Drag Reducing Devices: Three Case Studies', SAE Paper No. 870717, Detroit, USA.

Wheeler, G.O. 1991. Low Drag Vortex Generators, U.S. Patent No. 5,058,837. U.S. Department of Commerce, Washington DC.

Williamson, C.H.K. 1996.Three Dimensional Vortex Dynamics in Bluff Body Wakes,. Annual Review of Fluid Mechanics, 28: 477-539.

Zulfaa, M.K. and Antonio, F. 2010. Fuel savings on a heavy vehicle via aerodynamic drag reduction, Transportation Research Part D: Transport and Environment, 15(5): 275-284.